

## APPLICATION OF AIRBORNE DATA TO MONITOR URBAN INFRASTRUCTURE OBJECTS

O. Brovkina<sup>1\*</sup>, D. Kopkáně<sup>1</sup>, M. Polák<sup>2</sup>, A. Bednařík<sup>1</sup>, J. Hanuš<sup>1</sup>

<sup>1</sup> Global Change Research Institute of Czech Academy of Sciences, 603 00 Brno, Bělidla 4a - brovkina.o@czechglobe.cz

<sup>2</sup> Czech Environmental Information Agency (CENIA), 101 00 Praha, Moskevská 1523/63

**KEY WORDS:** Hyperspectral, FLIS, Asbestos-cement roof, Municipal solid waste landfill, Perceived temperature.

### ABSTRACT:

The paper demonstrates the application of hyperspectral data of Flight Laboratory of Imaging Systems (FLIS, <https://olc.czechglobe.cz/en>) to participate in three practical tasks of urban environment in the Czech Republic: 1/identification of asbestos-cement roofs on buildings; 2/monitoring of thermal regime of municipal solid waste landfill, and 3/estimation of perceived temperature in different parts of the city. These applications benefited from the airborne hyperspectral methods' ability to collect detailed spectral information, assess material composition, and extract biophysical parameters.

### 1. INTRODUCTION

The environmental impact of urban infrastructure objects refers to the potential or actual negative effects on the air, water, soil, flora, fauna, and human health. The impact may be temporary or permanent and can include soil erosion (Polovina et al., 2021), habitat destruction (Dubey et al., 2023), noise pollution (Chiarini et al., 2020), water pollution (Strokal et al., 2021), air pollution (Goyal et al., 2021), and greenhouse gas emissions (Isinkaralar et al., 2023). With the steady expansion of urban areas there is the increasing demand for efficient monitoring of urban infrastructure objects. Airborne remote sensing offers data and methods for a such applications.

Airborne remote sensing has emerged as a rapidly growing field with significant interest for monitoring urban objects (Liu et al., 2017; Zhao et al., 2019; Siddiqui et al., 2022). Airborne hyperspectral data in visible and near infrared (VNIR), short-wave infrared (SWIR), long-wave or thermal infrared (LWIR) region of the electromagnetic spectrum is a promising technology for monitoring the physical and functional features of objects of urban infrastructure to identify or prevent their negative impact.

Asbestos was commonly used in roofing materials in the past due to its fire-resistant properties and duration. However, asbestos is now recognized as a hazardous material, as inhalation of its fibers can significantly increase the risk of developing asbestos-related diseases. Bassani et al. (2007) described a systematic procedure for recognizing corrugated asbestos-cement roofing sheets and evaluating their deterioration status related to the asbestos fiber air dispersion. To develop this procedure, authors made field and laboratory measurements and acquired airborne MIVIS hyperspectral data covering industrial sites in Italy. APEX hyperspectral airborne imagery was classified to discriminate asbestos-cement roofing in the area of Karpacz, Poland (Krówczyńska et al., 2016). Yu et al. (2022) found that aerial hyperspectral scanners were a suitable tool to provide the significant bandwidth information needed to separate the asbestos-cement corrugated roofing tiles from cement roofing tiles in Taiwan.

Landfilling is a widely used and a relatively low demand method of municipal solid waste (MSW) disposal in most European

countries. Landfilling raises a number of environmental concerns, one of them is release of methane (CH<sub>4</sub>) from the ground surface, which contribute to greenhouse gas emissions and global warming (Cusworth et al., 2020). Intense decomposition of organic matter associated with methane production cause localized areas of increased temperature, which can be detected using airborne thermal imagery. Beaumont et al. (2014) used airborne FLIR SC7600-BB camera operating in the mid-wave infrared MWIR range (3.5-6 μm) to identify thermal anomalies present on multiple landfills. The importance of thermal monitoring of MSW landfills is emphasized in the review study (Sliushar et al., 2022), where about a quarter of the publications focus on estimation of the emissions of landfill gas or its individual components, mainly methane, using unmanned aerial vehicles. Significant thermal anomalies were identified during airborne thermal flights (Tanda et al., 2020), and thermal images were processed to obtain a rough estimation of the associated methane leakages.

Urban areas tend to have higher temperatures compared to their surrounding rural areas due to the urban heat island effect (Sangiorgio et al., 2020). This phenomenon arises from factors such as increased heat absorption and retention in built-up surfaces, reduced vegetation cover, and anthropogenic heat generation. Estimating perceived temperature allows for a comprehensive evaluation of the urban heat island effect's impact on human comfort. Airborne remote sensing helps in perceived temperature estimation to identify parts of the city that are particularly hot or uncomfortable for people to be in. Thermal airborne data are effectively utilized for capturing the spatial variations in surface temperature and thermal properties across the cityscape (Jin et al., 2021). Visible and near-infrared airborne hyperspectral data incorporate in other relevant factors, including land cover (Michel et al., 2021) and vegetation indices, enhances the estimation accuracy of thermal perception in urban environments.

The paper demonstrates the application of hyperspectral (HS) data of Flight Laboratory of Imaging Systems (FLIS, <https://olc.czechglobe.cz/en>) to participate in three practical tasks of urban environment in the Czech Republic: 1/identification of asbestos-cement roofs on buildings; 2/monitoring of thermal regime of municipal solid waste (MSW) landfill, and

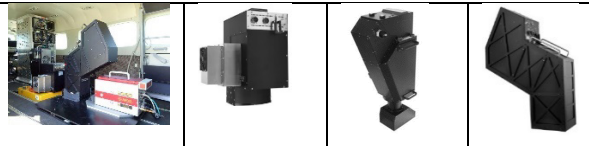
\* Corresponding author

3/estimation of perceived temperature in different parts of the city.

## 2. DATA AND METHODS

### 2.1 The Flying Laboratory of Imaging Systems

*Airborne sensors description.* The Flying Laboratory of Imaging Systems (FLIS) consists of an airborne carrier, imaging spectroradiometers and a laser scanner using for the various application (Brovkina et al. 2021). Photogrammetric airplane Cessna 208B Grand Caravan with two hatches serves as an airborne carrier. The basic sensor equipment consists of HS sensors CASI-1500, SASI-600 and TASI-600, produced by company Itres. Basic specifications are given in Table 1. These sensors are push broom scanners that scan the area of interest by individual rows. All HS sensors are equipped with custom-made sensing chips to ensure higher the so-called "full well capacity" of the detector allowing a higher range of measured signal without saturation. Greater dynamic range allows easier detection of the objects scanned.

			
Sensor	CASI - 1500	SASI - 600	TASI - 600
Spectral domain	VNIR	SWIR	LWIR
Spectral range [nm]	380 - 1050	950 - 2450	8000 - 11000
Number of spatial pixels	1500	600	600
Max. spectral resolution [nm]	3.2	15	110
FOV [°]	40	40	40
Spatial resolution [m]	0.5 - 2.0	1.25 - 5.0	1.25 - 5.0

**Table 1.** Basic technical specifications of the FLIS hyperspectral system. VNIR - visible and near infrared, SWIR - short-wave infrared, LWIR - long-wave infrared.

The scanners acquire data simultaneously. The aircraft is equipped with other devices and systems to improve the quality of the scanned data and to acquire auxiliary data for the final processing (the navigation system, gyroscopic platform, etc.). The current position and location of the aircraft (in three axes) is monitored using the GNSS/IMU POS AV inertial navigation unit. The data acquired by the hyperspectral sensor are synchronized with the signal from the GNSS/IMU unit and recorded into the acquisition computer.

*Data pre-processing.* The pre-processing of VNIR and SWIR data includes radiometric, geometric, and atmospheric corrections. The basic radiometric correction procedure consists in subtracting dark current and converting raw values scanned by the sensor (DN – digital numbers) into physically defined units of radiance. Radiometric corrections of measured data are carried out in RadCorr (Itres Ltd) using laboratory-determined calibration parameters that are determined for each pixel of the sensor matrix. The values of the final image data are given in radiometric units [ $\mu\text{W cm}^{-2} \text{sr}^{-1} \text{nm}^{-1}$ ] multiplied by 1000. Georeferencing is performed by means of parametric geocoding using data acquired by the GNSS/IMU unit and digital terrain model in GeoCor (Itres ltd.) program. In one single step, geometric corrections, orthorectification and georeferencing of

data is performed. Atmospheric correction is based on radiative transfer model (MODTRAN), enabling the calculation of absolute reflection without the need for prior knowledge of surface reflective properties. The resulting atmospherically corrected data are expressed in reflectance values at surface level. Pre-processing of thermal HS data includes atmospheric correction using MODTRAN and calculations of temperature characteristics using Temperature and Emissivity Separation algorithm (TES) (Pivovarnik et al., 2017).

### 2.2 Identification of asbestos-cement roofs on buildings

*Data acquisition.* HS data of FLIS were acquired for two Czech municipalities (Vysoké Popovice, 25.09.2021; Šošůvka, 29.08.2019) in VNIR, SWIR, and LWIR bands of electromagnetic spectrum (Table 1, [www.czechglobe.cz](http://www.czechglobe.cz)). Ground truth data were collected in the municipalities after an airborne campaign.

*Data processing.* The first approach was the Spectral Analyst method, wherein spectra of building roofs from airborne HS VNIR and SWIR data were compared with laboratory spectra from a specific sample with an unknown curve. The result was a probability value of the asbestos-cement spectrum occurring in the image pixel. The second approach was a supervised classification. The Registry of territorial identification, addresses and real estate (RUIAN) data, which was validated over the orthophoto of the State Administration of Land Surveying and Cadastre (ČÚZK) to create roofs mask. The process of airborne HS data normalization and residual noise reduction was performed using Minimum Noise Fraction transformation. Then, the pixel spectra of pure materials were found using pixel purity index with a setting of 10,000 iterations and a threshold of 2.5 standard deviations. Next, the end-members were selected as inputs to the classification with the Spectral Angle Mapper (SAM) method.

### 2.3 Monitoring of thermal regime of municipal solid waste landfill

*Data acquisition.* VNIR, SWIR, and LWIR HS data of FLIS were acquired 31.8.2022 at 10:00 CET and 3.12.2022 at 20:30 CET for the municipal solid waste landfill close to Brno city. Landfill objects surface temperature using a portable handheld infrared thermometer and concentration and fluxes of  $\text{CH}_4$  using a soil chamber connected to a portable greenhouse gas analyzer (Picarro GasScouter G4301, Picarro, CA, USA) were measured simultaneously with summer airborne data acquisition.

*Data processing.* The spectra profile of waste, mixture of waste with soil, and mixture of waste with vegetation from airborne VNIR and SWIR HS data were analysed to detect  $\text{CH}_4$  absorption features in several landfill parts. Methane indices (Xiao et al., 2020; Thorpe et al., 2021) incorporating specific narrow spectral SWIR regions (1630 - 1690 nm, 2100 – 2300 nm) were calculated to indicate the presence of  $\text{CH}_4$  "hot spots" on the landfill. The surface temperature of the landfill from airborne LWIR data was validated with surface temperature measurements on the landfill and mapped to identify locations with extremely high surface temperature. The  $\text{CH}_4$  emissions from landfill based on soil chamber measurements were calculated using a linear fit of the  $\text{CH}_4$  concentration change over time (3 min) for all chamber positions, and used for validation of  $\text{CH}_4$  "hot spots" from airborne SWIR data.

### 2.4 Estimation of perceived temperature in different parts of the city

*Data acquisition.* HS VNIR, SWIR, and LWIR data of FLIS were acquired 31.8.2019 between 10:45 to 14:30 CET for the Brno city. The air temperature was recorded at multiple monitoring

stations including high standard measurements by Czech Hydrometeorological Institute (<https://www.chmi.cz>).

**Data processing.** Firstly, the study area was classified into buildings, trees, paved and unpaved locations using HS VNIR and SWIR data. Secondly, the surface temperature was assigned for each class from HS LWIR data. Thirdly, a proxy air temperature was determined using the LWIR data, and it was corrected based on the degree of insolation using typical ground-based measurements. The accuracy of this correction was around 1 K. Finally, the perceived temperature was estimated based on the urban structure and the proxy air temperature with an accuracy of around 3 K.

### 3. RESULTS AND DISCUSSION

#### 3.1 Identification of asbestos-cement roofs on buildings

The accuracy of asbestos-cement roofs identification was 68 % using supervised classification with SAM method. The Spectral Analyst method demonstrated a 91% probability of asbestos occurrence validated using ground truth data. An improvement in identification of asbestos-cement roofs up to an accuracy of 96% was achieved by adding to the analysis the roof surface temperature and emissivity extracted from airborne HS TIR data (Figure 1).



**Figure 1.** Example of asbestos-cement roofs identification from airborne hyperspectral data using Spectral Analyst method (left) and Spectral Angle method (right).

Results of the airborne HS data application potentially can be interesting for organizations involved in the improvement of settlements, in architectural planning and environmental protection.

#### 3.2 Monitoring of thermal regime of municipal solid waste landfill

The surface temperature “hot spots” in several locations of the landfill body were more than two times higher than surface temperature of the surrounding vegetation (a proxy of “background temperature”). Maximum CH<sub>4</sub> concentrations and emissions were around 100 ppm and 5.9 g m<sup>-2</sup> d<sup>-1</sup>, respectively, in several locations of the landfill which spatially coincided with the locations of surface temperature “hot spots” on the landfill thermal map (Figure 2).

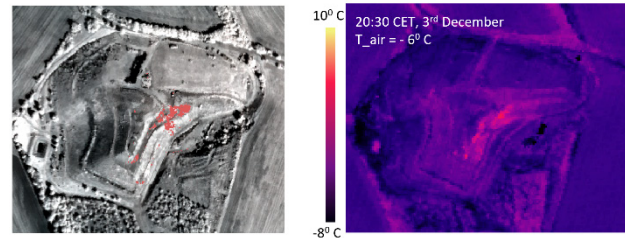


**Figure 2.** On the top: municipal solid waste landfill, view from the ground. *In situ* measurements of surface CH<sub>4</sub> concentration and fluxes and surface temperature. Below to the left: methane point sources from airborne shortwave infrared data (are marked with red). Below to the right: map of landfill surface temperature from airborne thermal data.

Airborne HS LWIR data potentially may be effective also in identifying low-level methane emissions. Additional study is required to further investigate the use of airborne data in landfill application.

#### 3.3 Estimation of perceived temperature in different parts of the city

Mapping the perceived temperature in the city can be performed at a detailed level, down to a single street, thanks to the high spatial resolution of the airborne data used (Figure 3). Moreover, the combination of airborne sensors allows for in-depth analysis by utilizing city land cover classification. Such a level of insight is currently not possible with satellite data due to its coarse spatial resolution in the thermal region (more than 50 m).

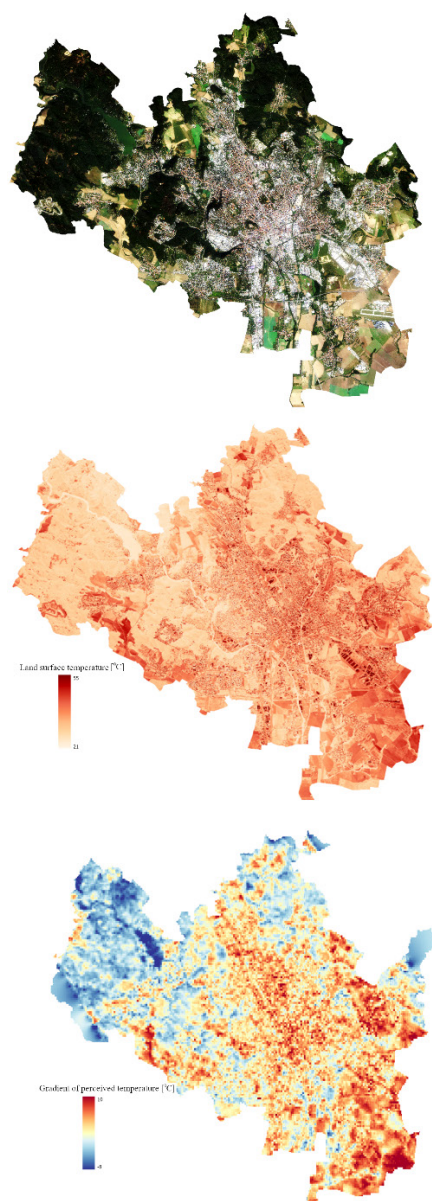


**Figure 3.** From top to bottom: orthophoto, map of land surface temperature, map of gradient of perceived equivalent temperature of Brno city. These maps were generated using airborne data acquired on August 31, 2019, between 10:45 and 14:30 CET.

The proposed methodology highlights the heat island phenomenon of the city with detail down to the level of individual streets and blocks.

## CONCLUSIONS

Airborne hyperspectral methods have a significant potential for monitoring urban objects. The paper demonstrated the methods application in several areas, including the identification of asbestos-cement roofs, monitoring of thermal regime of MSW landfills, and estimation of perceived temperature in various parts of the city. These applications benefited from the airborne hyperspectral methods' ability to collect detailed spectral information, assess material composition, and extract biophysical parameters. Such capabilities provide valuable information for urban planning, environmental assessment, and resource management.

## ACKNOWLEDGEMENTS

This work was supported by the Technology Agency of the Czech Republic grant number SS06020164, and by the Ministry of Education, Youth and Sports of CR within the CzeCOS program, grant number LM2023048.

## REFERENCES

Bassani, C., Cavalli, R. M., Cavalcante, F., Cuomo, V., Palombo, A., Pascucci, S., Pignatti, S. 2007. Deterioration status of asbestos-cement roofing sheets assessed by analyzing hyperspectral data. *Remote Sensing of Environment*, 109.

Beaumont, B., Radoux, J., Defourny, P. 2014. Assessment of airborne and spaceborne thermal infrared remote sensing for detecting and characterizing landfills. *WIT Transactions on Ecology and the Environment*, 180, 237-248. 10.2495/WM140201.

Brovkina, O., Hanuš, J., Novotný, J. 2021. Airborne remote sensing for forest inventory attributes assessment: experience of Flying Laboratory of Imaging Systems (FLIS) in the Czech Republic, IOP Conference Series: Earth and Environmental Science.

Chiarini, B., D'Agostino, A., Marzano, E., Regoli, A. 2020. The perception of air pollution and noise in urban environments: A subjective indicator across European countries, *Journal of Environmental Management*, 263, 110272, ISSN 0301-4797, <https://doi.org/10.1016/j.jenvman.2020.110272>.

Cusworth, D., Duren, R. M., Thorpe, A. K., Tseng, E., Thompson, D. et al. 2000. Using remote sensing to detect, validate, and quantify methane emissions from California solid waste operations. *Environmental Research Letters*, 15: 054012.

Dubey, R.S., Kalyan, S., Pathak, B. 2023. Impacts of Urbanization and Climate Change on Habitat Destruction and Emergence of Zoonotic Species. In: Pathak, B., Dubey, R.S. (eds) *Climate Change and Urban Environment Sustainability. Disaster Resilience and Green Growth*. Springer, Singapore. [https://doi.org/10.1007/978-981-19-7618-6\\_17](https://doi.org/10.1007/978-981-19-7618-6_17).

Goyal, P., Gulia, S., Goyal, S. K. 2021. Identification of air pollution hotspots in urban areas - An innovative approach using monitored concentrations data. *Sci Total Environ*. doi: 10.1016/j.scitotenv.2021.149143.

Isinkaralar, O. 2023. Bioclimatic comfort in urban planning and modeling spatial change during 2020–2100 according to climate change scenarios in Kocaeli, Türkiye. *Int. J. Environ. Sci. Technol.* <https://doi.org/10.1007/s13762-023-04992-9>.

Krówczynska, M., Wilk, E., Pabjanek, P., Zagajewski, B., Meuleman, K. 2016. Mapping asbestos-cement roofing with the use of APEX hyperspectral airborne imagery: Karpacz area, Poland – a case study. *Miscellanea geographica – regional studies on development*, 20 (1). DOI: 10.1515/mgrsd-2016-0007.

Liu, L., Coops, N. C., Aven, N. W., Pang, Y. 2017. Mapping urban tree species using integrated airborne hyperspectral and LiDAR remote sensing data. *Remote Sensing of Environment*, 200: 170-182, ISSN 0034-4257, <https://doi.org/10.1016/j.rse.2017.08.010>.

Pivovarník, M., Khalsa, S. J. S., Jiménez-Muñoz, J. C., Zemek, F. 2017. Improved temperature and emissivity separation algorithm for multispectral and hyperspectral sensors, in *IEEE Transactions on Geoscience and Remote Sensing*, 55 (4), 1944-1953, doi: 10.1109/TGRS.2016.2631508.

Polovina, S., Radic, B., Ristic, R., Kovačević, J., Milčanović, V., Živanović, N. 2021. Soil Erosion Assessment and Prediction in Urban Landscapes: A New G2 Model Approach. *Applied Sciences*, 11. 1-20. 10.3390/app11094154.

Rodriguez Potes, L., Hanrot, S., Dabat, M. A., Izard, J. L. 2013. Influence of trees on the air temperature in outdoor spaces according to planting parameters: the case of the city of Aix-en-Provence in France. *WIT Transactions on Ecology and the Environment*, 173, 291-298. 10.2495/SDP130251.

Sangiorgio, V., Fiorito, F., Santamouris, M. 2020. Development of a holistic urban heat island evaluation methodology. *Sci Rep.*, 10, 17913. <https://doi.org/10.1038/s41598-020-75018-4>.

Sidiqui, P., Roös, P.B., Herron, M. *et al.* 2022. Urban Heat Island vulnerability mapping using advanced GIS data and tools. *J Earth Syst Sci*, **131**, 266. <https://doi.org/10.1007/s12040-022-02005-w>.

Sliusar, N., Filkin, T., Huber-Humer, M., Ritzkowski, M. 2022. Drone technology in municipal solid waste management and landfilling: A comprehensive review. *Waste Management*, 139, <https://doi.org/10.1016/j.wasman.2021.12.006>.

Strokal, M., Bai, Z., Franssen, W. 2021. Urbanization: an increasing source of multiple pollutants to rivers in the 21st century. *Urban Sustain*, 24. <https://doi.org/10.1038/s42949-021-00026-w>.

Tanda, G., Balsi, M., Fallavollita, P., Chiarabini, V. 2020. A UAV-based thermal-imaging approach for the monitoring of urban landfills. *Inventions*, 5 (55). 10.3390/inventions5040055.

Thorpe, A. K., O'Handley, C., Emmitt, G. D., DeCola, P. L., Hopkins, F. M., Yadav, V., Guha, A., *et al.* 2021. Improved methane emission estimates using AVIRIS-NG and an Airborne Doppler Wind Lidar, *Remote Sensing of Environment*, 266, <https://doi.org/10.1016/j.rse.2021.112681>.

Xiao, C, B. Fu, H. Shiu, Z. Guo, and J. Zhu. 2020. Detecting the sources of methane emission from oil shale mining and processing using airborne hyperspectral data. *Remote Sensing*, 12 (3): 537.

Yu, T.-T., Lin, Y.-C., Lan, S.-C., Yang, Y.-E., Wu, P.-Y., Lin, J.-C. 2022. Mapping Asbestos-Cement Corrugated Roofing Tiles with Imagery Cube via Machine Learning in Taiwan. *Remote Sens.*, 14, 3418. <https://doi.org/10.3390/rs14143418>.

Zhao, C., Jensen, J., Weng, O., Currit, N., Weaver, R. 2019. Application of airborne remote sensing data on mapping local climate zones: Cases of three metropolitan areas of Texas, U.S. *Computers, Environment and Urban Systems*, 74: 175-193, <https://doi.org/10.1016/j.compenurbsys.2018.11.002>.